

Fluorescence quenching in tip-enhanced nonlinear optical microscopy

John T. Krug II, Erik J. Sánchez, and X. Sunney Xie

Citation: [Applied Physics Letters](#) **86**, 233102 (2005); doi: 10.1063/1.1935769

View online: <http://dx.doi.org/10.1063/1.1935769>

View Table of Contents: <http://scitation.aip.org/content/aip/journal/apl/86/23?ver=pdfcov>

Published by the [AIP Publishing](#)

Articles you may be interested in

[Tip-enhanced sub-diffraction fluorescence imaging of nitrogen-vacancy centers in nanodiamonds](#)

Appl. Phys. Lett. **102**, 013102 (2013); 10.1063/1.4773364

[Tip-enhanced two-photon excited fluorescence microscopy with a silicon tip](#)

Appl. Phys. Lett. **94**, 193112 (2009); 10.1063/1.3138132

[Enhancement of two-photon excited fluorescence in two-dimensional nonlinear optical polymer photonic crystal waveguides](#)

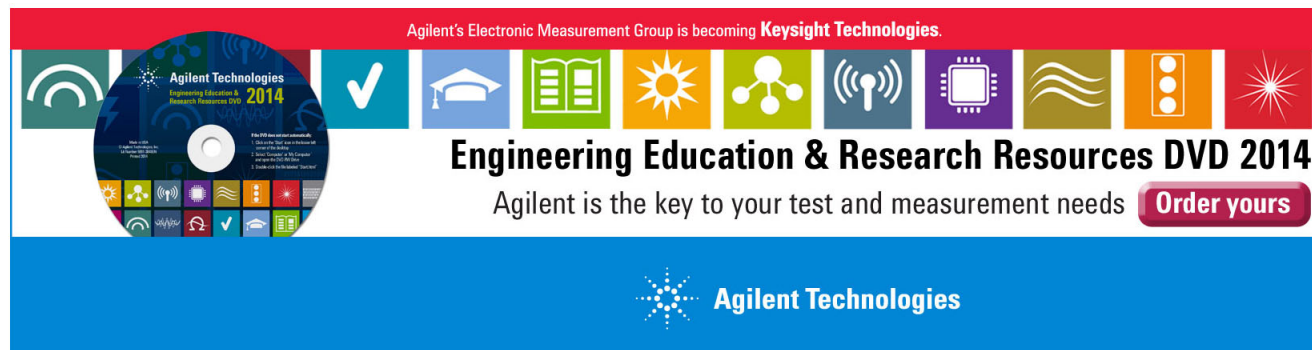
Appl. Phys. Lett. **93**, 111110 (2008); 10.1063/1.2985902

[Tip-enhanced fluorescence imaging of quantum dots](#)

Appl. Phys. Lett. **87**, 183101 (2005); 10.1063/1.2115073

[Application of tip-enhanced microscopy for nonlinear Raman spectroscopy](#)

Appl. Phys. Lett. **84**, 1768 (2004); 10.1063/1.1647277

This is a promotional banner for Agilent Technologies' Engineering Education & Research Resources DVD 2014. At the top, a red bar contains the text 'Agilent's Electronic Measurement Group is becoming Keysight Technologies.' Below this, a row of ten colorful icons represents various engineering fields: a green arc, a blue checkmark, a blue graduation cap, a green book, a yellow sun, a green network diagram, a blue antenna, a purple microchip, a green wave, an orange circuit board, and a red starburst. To the left of these icons is a circular image of the DVD itself, which features the same icons and the text 'Agilent Technologies Engineering Education & Research Resources DVD 2014'. Below the icons, the text 'Engineering Education & Research Resources DVD 2014' is written in a large, bold, black font. Underneath this, a smaller line of text reads 'Agilent is the key to your test and measurement needs', followed by a red button with the white text 'Order yours'. The entire banner is set against a blue background with the Agilent Technologies logo and name at the bottom.

Fluorescence quenching in tip-enhanced nonlinear optical microscopy

John T. Krug II

Department of Chemistry and Chemical Biology, Harvard University, Cambridge, Massachusetts 02138

Erik J. Sánchez

Department of Physics, Portland State University, Portland, Oregon 97207

X. Sunney Xie^{a)}

Department of Chemistry and Chemical Biology, Harvard University, Cambridge, Massachusetts 02138

(Received 11 November 2004; accepted 13 April 2005; published online 31 May 2005)

We describe the theoretical treatment of fluorescence quenching in tip-enhanced nonlinear optical microscopy (TENOM). Finite difference time domain simulations demonstrate that while sharp pyramidal probes yield fluorescence signal enhancement that decays monotonically as a function of probe-fluorophore distance, more commonly used conical probes cause more complex image contrast. Fluorescence quenching can thus explain the halo-type images that are sometimes observed in TENOM. Formation of a dielectric spacer layer on the TENOM probe should alleviate the complications associated with quenching. © 2005 American Institute of Physics. [DOI: 10.1063/1.1935769]

Tip-enhanced nonlinear optical microscopy (TENOM) uses the enhanced and confined optical field at the apex of a sharp noble metal probe as a two-photon fluorescence excitation source.¹ This approach yields optical images with sub-20 nm spatial resolution.² However, TENOM has primarily been used for the study of molecularly aggregated systems for which fast energy transfer relaxes excitation energy large distances from the probe.^{3,4} Fast energy transfer therefore mitigates the effects of fluorescence quenching by the gold or silver probes in these experiments.

However, fluorescence quenching will be important in TENOM of isolated fluorophores. Several groups have reported the use of metal-coated atomic force microscopy probes for fluorescence imaging.^{5–7} In these experiments, understanding the quenching properties of the three-dimensional (3D) nanoscale metal probe is of utmost importance. While the Chance, Prock, Silbey (CPS) theory⁸ can be used to treat dipole quenching by flat metal mirrors, the curvature of apertureless near-field scanning optical microscopy (NSOM) probes is on the same scale as the experimental probe-fluorophore separation. As such, the analytically soluble CPS theory cannot be applied in a straightforward fashion.

We present the application of 3D finite difference time domain (FDTD) electromagnetic calculation^{9,10} coupled to the CPS theory for the understanding of optical contrast in TENOM of isolated fluorophores. Combined electric-field enhancement and fluorescence quantum yield calculations allow us to determine the signal enhancement expected for arbitrary probe-fluorophore geometries. When rounded conical probes are used, the signal enhancement for the dipole peaks at an experimentally significant distance from the probe apex. The drop in signal at zero separation explains the appearance of a halo-type optical contrast. This complicated contrast can be avoided by selecting probes designed for optimal field enhancement or by maintaining some minimum probe-fluorophore separation.

In order to calculate the TENOM signal enhancement for a given probe-fluorophore geometry, one must calculate the excitation enhancement at $\lambda=825$ nm and the dipole quantum yield at $\lambda=450$ nm. As previously reported, we calculate the electric-field enhancement factor by illuminating the geometries of interest with 825 nm plane waves in 3D FDTD simulations¹¹ (see Fig. 1). The position-dependent fluorescence quantum yield, $\phi_{\text{eff}}=k_r/(k_r+k_{\text{nr}})$, is calculated by simulating a Hertzian dipole in FDTD. This is achieved by calculating the amplitude and phase of the dipole radiated electric field reflected back to the dipole position by the probe, and determining the effect of the metal nanoprobe on the power radiated by the dipole.¹² If $k=k_r+k_{\text{nr}}$ in the presence of the probe, k_0 is the dipole decay rate in the absence of the probe, and W/W_0 is the relative power radiated by the dipole in the presence of the probe, then the position and wavelength-dependent effective quantum yield can be calculated

$$\frac{k}{k_0} = 1 + \frac{6\pi q \epsilon \epsilon_0}{\mu_0 k^3} E_R \sin \phi_R,$$

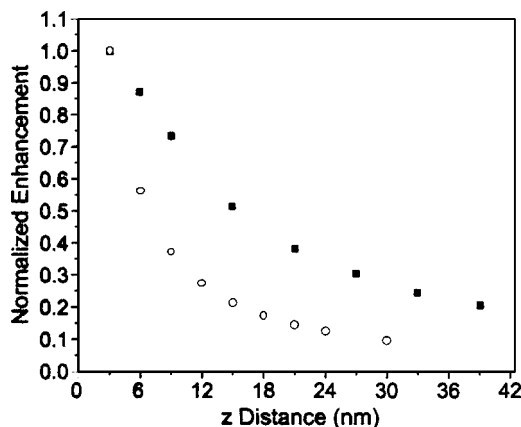


FIG. 1. Normalized electric field enhancement for the conical probe (filled squares) and the right trigonal pyramidal probe (empty circles) at $\lambda=825$ nm as a function of distance from the probe apex along the z axis is calculated with FDTD. The pyramidal probe confines the field more strongly than does the conical probe.

^{a)} Author to whom correspondence should be addressed; electronic mail: xie@chemistry.harvard.edu

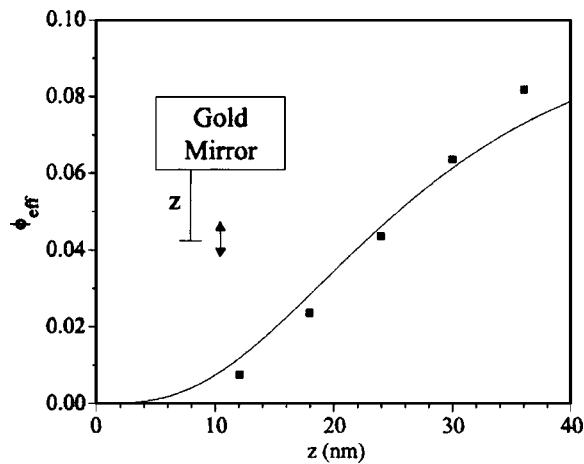


FIG. 2. FDTD (filled squares) and analytically calculated (via CPS theory, solid line) quantum yields for dipoles near gold mirrors. The dipole is polarized normal to the gold-air interface, and the interface-dipole distance (z) is varied. The FDTD calculated quantum yields match the analytical results reasonably well to distances of approximately 40 nm.

$$\phi_{\text{eff}} = \frac{k_r}{k_r + k_{\text{nr}}} = \frac{W/W_0}{k/k_0}.$$

Here, k_r is the radiative decay rate, and k_{nr} is the nonradiative decay rate. The quantum yield of the free dipole, q , is

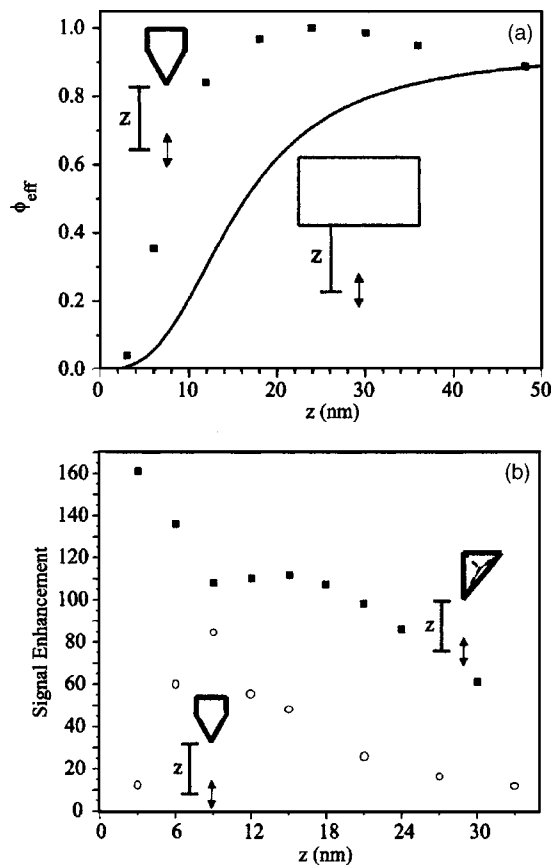


FIG. 3. (a) The effective quantum yield of a dipole emitting at $\lambda=450$ nm clearly depends on the geometry of the probe, as the analytically calculated quantum yield for the dipole (solid line) near a mirror is significantly different from that calculated with FDTD (filled squares) for a dipole near a conical gold probe. (b) Signal enhancement is calculated with FDTD for pyramidal and conical probes. While the pyramidal probe (filled squares) generates the strongest signal enhancement at the smallest calculable probe-dipole distance (3 nm), the conical probe (empty circles) yields signal enhancement that peaks 9 nm from the probe apex.

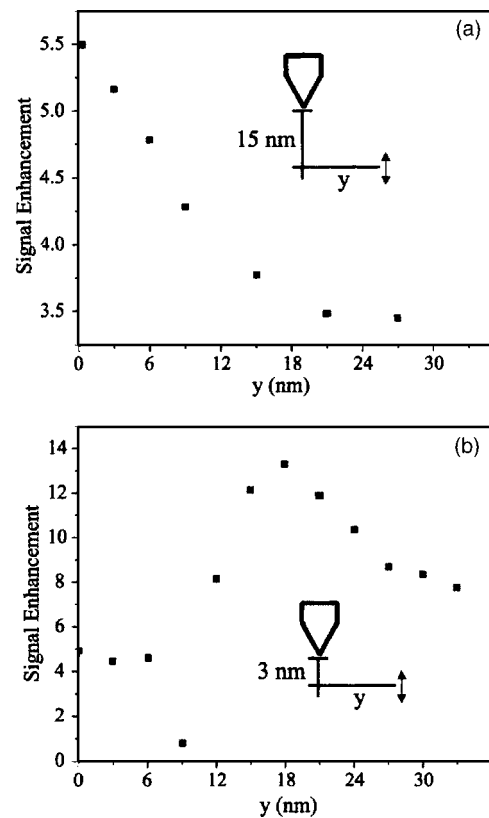


FIG. 4. (a) Signal enhancement cross section for a $\lambda=450$ nm emitting dipole separated by 15 nm from the probe apex along the z axis. The peak signal enhancement occurs at the smallest lateral displacement. (b) When the dipole is only 3 nm from the conical probe apex, the peak signal enhancement occurs when the dipole is laterally displaced by 18 nm. This phenomenon explains the halo-type image contrast seen in TENOM imaging of isolated fluorophores.

assumed to be 1. \mathbf{k} is the wave vector for the dipole, and ϵ is the permittivity of the medium. The near-field generated signal enhancement (S) at a given position and wavelength is simply the product of the square of the electric-field intensity enhancement (G) and the effective quantum yield of the dipole

$$S \propto G^2 \phi_{\text{eff}}.$$

As in previous two-dimensional FDTD calculations of quenching by aperture NSOM probes, we simulate the quenching of fluorescence by a mirror in order to verify the accuracy of our calculations.¹² Simulated results are compared to those calculated via the analytical CPS theory (see Fig. 2). Proper treatment of the simulated material optical constants, in the near-IR and at 450 nm, allows us to accurately model quenching of dipoles normal to a gold mirror at distances of up to 50 nm. (Due to the fact that the dominant excitation field in our experiments is polarized normal to the probe, calculation of quenching for dipoles in other orientations is superfluous.)

Previous research into the quenching of fluorophores by metal-coated atomic force microscopy probes has used CPS calculation to provide a theoretical framework.⁶ However, our results clearly demonstrate that the behavior of dipoles in close proximity to conical TENOM probes is vastly different than that for dipoles near gold mirrors [see Fig. 3(a)]. The effective quantum yield for the dipole near the conical probe increases much more rapidly than does the quantum yield for the dipole near a mirror. At 12 nm interface-dipole separa-

tion, the quantum yield for the cone is roughly three times greater than that for the mirror. This discrepancy is intuitive, as the radius of curvature of the probe apex, 15 nm, is comparable to the probe-dipole distances. As the dipole moves away from the probe, the curvature of the probe becomes apparent. Only at minute distances will the probe appear to be planar from the dipole's point of view.

Furthermore, the shift from a conical to a pyramidal probe yields qualitative differences in signal enhancement [see Fig. 3(b)]. The quasi-infinite conical probe is experimentally common,^{1,2,13–15} while the finite right trigonal pyramidal probe has been shown to yield optimal field enhancement.¹¹ It is important to note that the pyramidal probe is terminated in a single 3 nm cubic cell rather than a 15 nm radius sphere. While the pyramid has its highest signal enhancement (161) at a probe-dipole distance of 3 nm (the smallest distance calculable in these simulations), the conical probe yields minimal signal enhancement (12) at the smallest separation. Conical probe signal enhancement peaks at 9 nm separation at 85 \times . This nonmonotonic distance dependence in signal enhancement causes halo-type optical contrast.

In order to test this theory, we calculated signal enhancement cross sections for the conical probe at two probe-dipole z displacements (see Fig. 4). When the dipole is 15 nm away from the conical probe apex in the z axis, the signal enhancement decays monotonically as a function of y displacement. Separating the dipole from the probe by 15 nm ensures that the signal is optimized when the probe is directly above the fluorophore, simplifying the image contrast. However, when the dipole is only separated from the probe by 3 nm in the z axis, the signal enhancement cross section is more complicated, with signal enhancement peaking at $\Delta y = 18$ nm. This dramatic difference explains the observed halo artifact in TENOM of isolated fluorophores.

We have demonstrated the use of 3D FDTD simulations for the explanation of fluorescence quenching and image formation mechanisms in the TENOM experiment. This FDTD approach provides a straightforward alternative to field expansion approaches, such as that of Novotny.¹⁶ While TENOM probes with optimal field enhancement can overcome low fluorescence quantum yields at small probe-dipole separations, more commonly used conical probes can easily result in images complicated by fluorescence quenching. Maintaining a minimum probe-fluorophore separation, as by application of a dielectric spacer layer¹⁷ on the probe apex, should simplify image interpretation in TENOM experiments.

¹L. Novotny, E. J. Sánchez, and X. S. Xie, *Ultramicroscopy* **71**, 21 (1998).

²E. J. Sánchez, L. Novotny, and X. S. Xie, *Phys. Rev. Lett.* **82**, 4014 (1999).

³M. L. Horng and E. L. Quitevis, *J. Phys. Chem.* **97**, 12408 (1993).

⁴D. A. Higgins and P. F. Barbara, *J. Phys. Chem.* **99**, 3 (1995).

⁵T. J. Yang, G. A. Lessard, and S. R. Quake, *Appl. Phys. Lett.* **76**, 378 (2000).

⁶W. Tragesinger, A. Kramer, M. Kreiter, B. Hecht, and U. P. Wild, *Appl. Phys. Lett.* **81**, 2118 (2002).

⁷Y. Kawata, C. Xu, and W. Denk, *J. Appl. Phys.* **85**, 1294 (1999).

⁸R. R. Chance, A. Prock, and R. Silbey, *Adv. Chem. Phys.* **37**, 1 (1978).

⁹A. Taflov and M. E. Brodwin, *IEEE Trans. Microwave Theory Tech.* **23**, 623 (1975).

¹⁰K. S. Kunz and R. J. Luebbers, *The Finite Difference Time Domain Method for Electromagnetics* (CRC Press, Boca Raton, FL, 1993).

¹¹J. T. Krug II, E. J. Sánchez, and X. S. Xie, *J. Chem. Phys.* **116**, 10895 (2002).

¹²R. X. Bian, R. C. Dunn, X. S. Xie, and P. T. Leung, *Phys. Rev. Lett.* **75**, 4772-5 (1995).

¹³L. Novotny, R. X. Bian, and X. S. Xie, *Phys. Rev. Lett.* **79**, 645 (1997).

¹⁴L. Novotny, M. R. Beversluis, K. S. Youngworth, and T. G. Brown, *Phys. Rev. Lett.* **86**, 5251 (2001).

¹⁵A. Hartschuh, E. J. Sánchez, X. S. Xie, and L. Novotny, *Phys. Rev. Lett.* **90**, 095503 (2003).

¹⁶L. Novotny, *Appl. Phys. Lett.* **69**, 3806 (1996).

¹⁷E. J. Sánchez, J. T. Krug II, and X. S. Xie, *Rev. Sci. Instrum.* **73**, 3901 (2002).